ASTFE
American Society
of Thermal and Fluids Engineers

4th Thermal and Fluids Engineering Conference (TFEC)
April 14–17, 2019
Las Vegas, NV, USA

TFEC-2019-27962

THERMAL AND HYDRAULIC PERFORMANCE OF LONGITUDINAL PERFORATED RECTANGULAR FINS WITH PERFORATION SHAPE AND SIZE VARIATIONS

Hamid Maleki[1], Mohammad Reza Safaei[2,*], Arturo S. Leon[2], Truong Khang Nguyen[3, 4]

[1]Department of Mechanical Engineering, Isfahan University of Technology, Isfahan, 84156-83111, Iran
[2]Department of Civil and Environmental Engineering, Florida International University, Miami, Florida, U.S.A.
[3]Division of Computational Physics, Institute for Computational Science, Ton Duc Thang University, Ho Chi Minh City, Vietnam
[4]Faculty of Electrical and Electronics Engineering, Ton Duc Thang University, Ho Chi Minh City, Vietnam

ABSTRACT

Improving heat transfer rate and reducing manufacturing costs are two significant objectives in the optimal design of heat sinks, which are used in electrical devices. Due to economic reasons in cooling applications, different methods were used to increase the efficiency of thermal devices such as creating perforations in fins, which reduces the volume of fins and increases thermal dissipation. In this study, an attempt was made to improve the thermal and hydraulic performance of fluid flow over a three-dimensional array of rectangular perforated fins with different perforations shapes and sizes. Finite volume method with the SIMPLE algorithm was applied to solve the incompressible laminar Navier-Stokes and energy equations. Flow and heat transfer characteristics were presented for Reynolds number (based on fin thickness) from 100 to 350 and a Prandtl number of 0.71 (air). In this study, the effects of perforation size and shape on the average Nusselt number, total drag force, and perforated fin effectiveness were assessed. The results of this investigation confirmed that for a constant heat transfer surface area, the highest values of perforated fin effectiveness and average Nusselt number are obtained for fins with circular perforations.

KEY WORDS: Heat transfer performance, Numerical simulation, Perforated fin, Fin weight.

1. INTRODUCTION

In recent years, due to economic reasons (savings in material and energy), considerable efforts have been made to develop methods for optimizing heat transfer equipment and hence achieve a better efficiency. Different methods were used to increase the efficiency of thermal devices and most of these involved application of extended surfaces [1] and adding nanomaterials for heat transfer enhancement [2-4]. One common approach to improve heat transfer in heat exchangers is the placement of fins which extend the heat transfer surface between the fluid and devices. Among Fins with different shapes, rectangular fins are more widely used in different thermal devices due to the simple production process. In this regard, Park and Chung [5] used a finite volume method to calculate flow and heat transfer features for an array of rectangular fins in a duct by altering the tip clearance and Prandtl number. Zadhoush et al. [6] employed the constructal theory to optimize the geometry of longitudinal and latitudinal rectangular fins. In another work, Ghorbani-Tari et al. [7] investigated the influence of blockage ratio on flow and heat transfer of a rectangular bluff body in a turbulent channel flow numerically. Mokhtari et al. [8] performed a numerical simulation to study the mixed convection of a three-dimensional channel with different configurations of rectangular fins in laminar and turbulent fluid flow.

*Corresponding Author: cfd_safaei@yahoo.com

Over the last few years and owing to the broad application of fins in various industries, the discussion of "fins optimization" has become important for many researchers. One of the best methods in fins optimization is to create perforations on the fins. In this method, it is possible to reduce fin weight as well as increase the heat transfer surface area, which satisfies simultaneously both objectives of fin optimization. Many researchers studied the flow and heat transfer performance of different thermal devices in the presence of perforated fins. In this regard, Maji et al. [9] numerically investigated flow and heat transfer through pin fins with various number and size of perforations. Their results showed that perforated fins have a higher heat transfer rate, compared to solid ones. Also, they found that increasing the size and number of perforations reduced the pressure drop. Chidambaram et al. [10] performed a numerical simulation to study plate fins with longitudinal rectangular perforations. They used a multi-objective optimization based on genetic algorithms and artificial neural networks to determine optimal parameters for minimizing the temperature of the base plate and maximizing the weight reduction of perforated fins. Shaeri and Bonner [11] experimentally analyzed the impact of laterally square perforations on flow and heat transfer of finned heat sinks for both laminar and turbulent flow regimes. They investigated the variation of thermal and flow characteristics under the influence of perforation size and porosity. Shaeri and Yaghoubi [12] conducted a numerical study on an array of rectangular fins with longitudinal perforations in the laminar flow regime. They showed that porosity (which indicates the ratio of perforations volume to the volume of the solid fin) is the most significant variable in perforated fins design. In another work, Shaeri and Jen [13] studied the effect of number and size of perforations in laminar flows through an array of perforated fins with the highest porosity reported by Shaeri and Yaghoubi [12]. Their results indicated that in constant porosity, fins with fewer perforations have better thermal performance than fins with numerous perforations.

In two previous studies [12, 13] only fins with rectangular perforations were studied. In the present investigation, an effort was made to improve the thermal and hydraulic performance of fluid flow over a three-dimensional array of rectangular perforated fins with different perforations shapes and fin surface area ratios between 1.85 and 2. The present work considers fins with three longitudinal perforations and four perforation shapes namely square, hexagonal, triangular and circular.

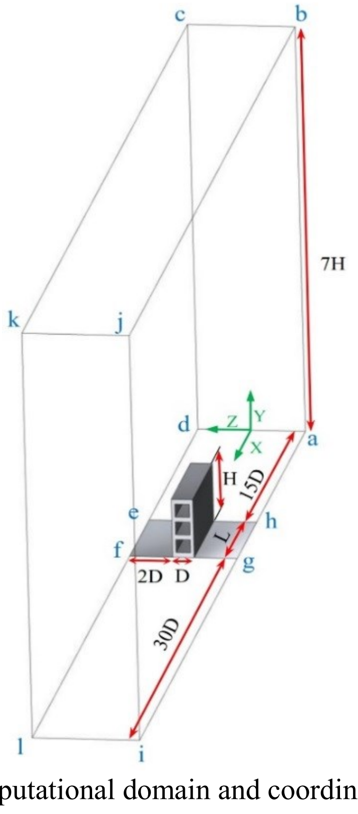

Fig. 1 Computational domain and coordinate system.

2. PROBLEM DESCRIPTION

In this study, due to the symmetry in fins array, only one fin is modeled. Fig. 1 displays the computational domain used in the present paper. This figure shows the entrance region as “abcd”, free stream surface as “bckj”, and exit plane as “ijkl”. Based on previous studies [12, 13], the dimension of the computational domain in upstream, downstream, Y and Z directions are chosen to be 15D, 30D, 7H, and 5D, respectively. The dimensions of fin are 24 mm×12 mm×4 mm for length (L) × height (H) × thickness (D). The temperature of the base plate (efgh) is 70 °C, and the free stream temperature is equal to 25 °C. Planes “abji” and “dckl” have symmetric boundary condition. Also no-slip and adiabatic conditions are applied to “adeh” and “gfli” planes. Flow and heat transfer characteristics are presented for Reynolds number (based on fin thickness) from 100 to 350 and Prandtl number of 0.71 (air). Fins with three longitudinal perforations are considered and four perforation shapes namely hexagonal, square, triangular and circular examined at various surface area ratios ($\sigma = 1.85$-2). Surface area ratio (σ) is the ratio of surface area of perforated fin divided by the same quantity for the solid fin. Moreover, fin material is assumed to be aluminum with thermal conductivity of 202 W/mK which is widely used in different heat sinks.

3. COMPUTATIONAL MODELING AND PROCEDURE

3.1. Energy and Flow Equations The three-dimensional incompressible, steady-state fluid flow in the laminar regime is represented via equations (1)-(3) [12, 13].

Continuity equation:

$$\frac{\partial u_i}{\partial X_i} = 0 \tag{1}$$

Momentum equation:

$$\rho u_j \frac{\partial u_i}{\partial X_j} = -\frac{\partial P}{\partial X_i} + \mu \frac{\partial^2 u_i}{\partial X_i^2} \tag{2}$$

Energy equation:

$$\rho C_p u_j \frac{\partial T}{\partial X_j} = K \frac{\partial^2 T}{\partial X_i \partial X_i} \tag{3}$$

To determine temperature field in the fin’s surfaces and perforation’s walls, the Fourier’s steady state heat conduction equation was solved in solid region simultaneously with convection in the fluid.

Table 1 Mesh convergence study for fin with square perforations (σ=1.95 and Re_D=250).

step	Grid (X, Y, Z)	average Nusselt number
1	120 × 54 × 30	2.23
2	148 × 70 × 38	2.41
3	185 × 90 × 48	2.50
4	208 × 102 × 56	2.52
5	230 × 116 × 60	2.52

3.2. Numerical Procedure A finite volume method (FVM) is used to solve the governing equations (1)-(3). Among the pressure and velocity coupling methods, the SIMPLE algorithm is employed. Also, the discretization of governing equations is performed using the second-order upwind scheme. The convergence criteria for the momentum and energy equations are considered to be 10^{-6} and 10^{-10}, respectively. In order to ensure the precision of the numerical solution, a mesh convergence study was performed, which results are presented in

Table 1. In the present study, structured hexahedron body-fitted meshing was used for all geometries. As shown in Table 1, five sets of meshes are examined. As shown in this table, by increasing the number of grid points in the domain from step 3 onwards, the variations in average Nusselt number become smaller than 1 percent. Therefore, it was deemed that the step 3 mesh with 185, 90 and 48 grid points in the X, Y, and Z directions, respectively, is accurate enough for the present simulation.

3.3. Parameter Definitions Here, the thermal and hydraulic performance of the fins is evaluated via the following parameters: average Nusselt number, perforated fin effectiveness (PFE) and total drag force. The PFE parameter is used to determine the increase in the heat transfer rate of perforated fins compared to the solid fins. This parameter can be defined as follows:

$$\text{PFE} = \frac{q_{pf} - q_{sf}}{q_{sf}} \times 100 \tag{4}$$

Where q_{sf} and q_{pf} represent the heat transfer rate of the solid fin and perforated fin, respectively. The expression for obtaining q_{f} is:

$$q_f = \sum_i h_i \Delta A_i (T_s - T_\infty) \tag{5}$$

Here T_s and T_∞ are fin surface and the free stream temperatures, respectively. The total drag force consists of two components, including the friction and pressure drag, calculated as follows:

$$F_D = F_F + F_P \tag{6}$$

$$F_F = \sum_i (\tau_w)_i \Delta A_i = \sum_i \mu \left(\frac{\partial u}{\partial n_i}\right)_s \Delta A_i \tag{7}$$

$$F_P = \left(-\sum_i P_i \Delta A_i\right)_{US} - \left(-\sum_i P_i \Delta A_i\right)_{DS} \tag{8}$$

Where τ_w is defined as local shear stress on fin and perforation surfaces. In Eq. (7), ΔA_i is associated with fin surfaces parallel to the flow direction, which contact with the fluid. This area includes both inside surface of perforations and outside surface of the fin. This value rises by increasing the size of perforations. On the other hand, ΔA_i in Eq. (8) is related to the frontal and posterior surface of the fin which is normal to the flow direction. This area is reduced in perforated fins and is further reduced by growing perforations size. Eq. (9) is used for calculating average Nusselt number:

$$\overline{Nu} = \frac{\bar{h} D}{K} \tag{9}$$

Where

$$\bar{h} = \frac{1}{A_T} \sum_i h_i \Delta A_i \tag{10}$$

In Eq. (10), the total fin area in contact with the fluid is taken as A_{T}, including inside surface of perforations plus outside surface of fins.

Table 2 Comparison of the average Nusselt number for the present results with those published by Shaeri and Yaghoubi [12] for a fin with three perforations.

Re	Shaeri and Yaghoubi [12]	present work
100	1.412	1.407
150	1.702	1.695
200	1.930	1.926
250	2.144	2.133
300	2.343	2.324
350	2.545	2.521

3.4. Validation Table 2 shows the comparison of the average Nusselt number for the present results with the numerical results of Shaeri and Yaghoubi [12]. This verification was performed for a rectangular fin with three square perforations which correspond to the porosity of 0.1665. As can be observed, the maximum difference between the present results and those obtained by reference [12] is less than 1%, which indicates that the present numerical scheme is accurate and reliable.

4. RESULTS AND DISCUSSION

In this investigation, a fin modifying method, namely perforated fin, is applied to improve the thermal and hydraulic performance of fluid flow over a three-dimensional array of rectangular fins. In this section, flow and heat transfer characteristics such as the Nusselt number, total drag force, and perforated fin effectiveness (PFE) under the influence of the Reynolds number, the shape of perforations and fin surface area ratio are examined.

Fig. 2(a and b) presents the variation of total drag force for various Reynolds numbers and fin surface area ratios (σ) and different perforation shapes. This figure indicates that the total drag force rise with the increase of the Reynolds number. Also, the impact of perforation shape on the total drag force values become more evident, with the Reynolds number increment. Comparison of different fins at various Reynolds numbers confirm that the highest and lowest total drag force is observed for solid fin and fin with circular perforations, respectively. Moreover, increasing the size of the perforations leads to a reduction of the total drag force; although, these variations are various for different shapes of perforations. This means that the total drag reduction for fins with circular perforations is more than other fins. However, fins with triangular perforations have the slightest change by resizing the perforations. A decrease in drag force means that the power of external force, for example, a fan, can be reduced. On the other hand, raising drag force results in higher fan power and energy; and consequently, a higher operating cost.

Fig. 3(a and b) displays the variation of average Nusselt number for various Reynolds numbers and fin surface area ratios (σ) and different perforation shapes. As it can be seen in Fig. 3(a), the highest average Nusselt number is obtained for a solid fin. Also among the tested perforated fins, the fins with circular perforations have the highest value of the average Nusselt number. Also, Fig. 3 shows that as the Reynolds number increases, the average Nusselt number difference between the solid fin and perforated fins decreases. In fact, by creating perforations on the fins, some of the air flow is directed into the perforations, which reduces the flow velocity around the fin. This process decreases the Nusselt number of perforated fins relative to a solid fin. By raising the Reynolds number and the size of the perforations, the flow velocity around the fin and inside the perforations is boosted which leads to an increase of the Nusselt number.

The impact of shape and size of perforations and also Reynolds number on perforated fin effectiveness (PFE) parameter are shown in Fig. 4. As shown in this figure, an increase of the Reynolds number and the size of the perforations lead to an increase in heat transfer rate for all tested fins. Also, fins with circular and triangular perforations show the best and worst thermal performance, respectively.

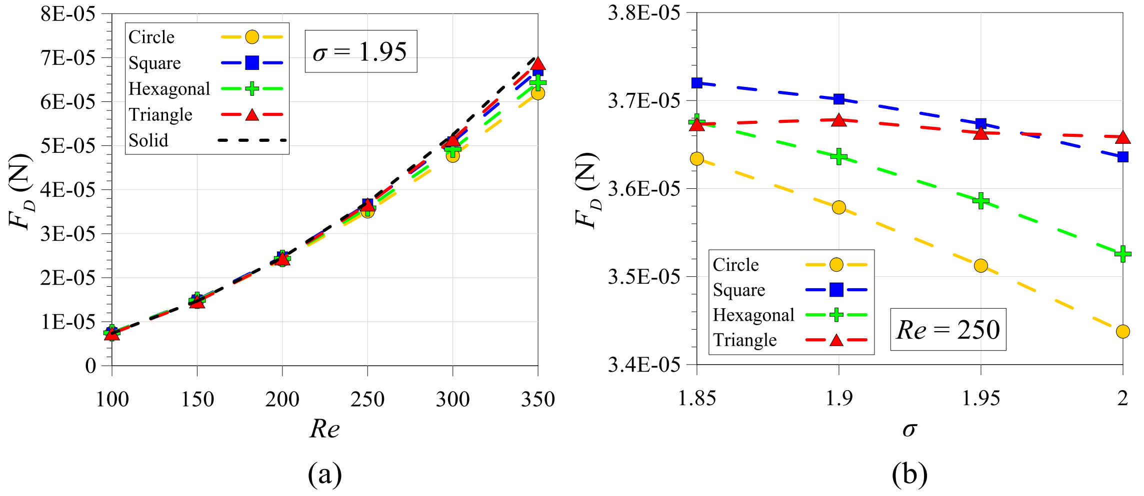

(a) (b)

Fig. 2 Variation of total drag force for different types of fins at various (a) Reynolds number and (b) surface area ratio.

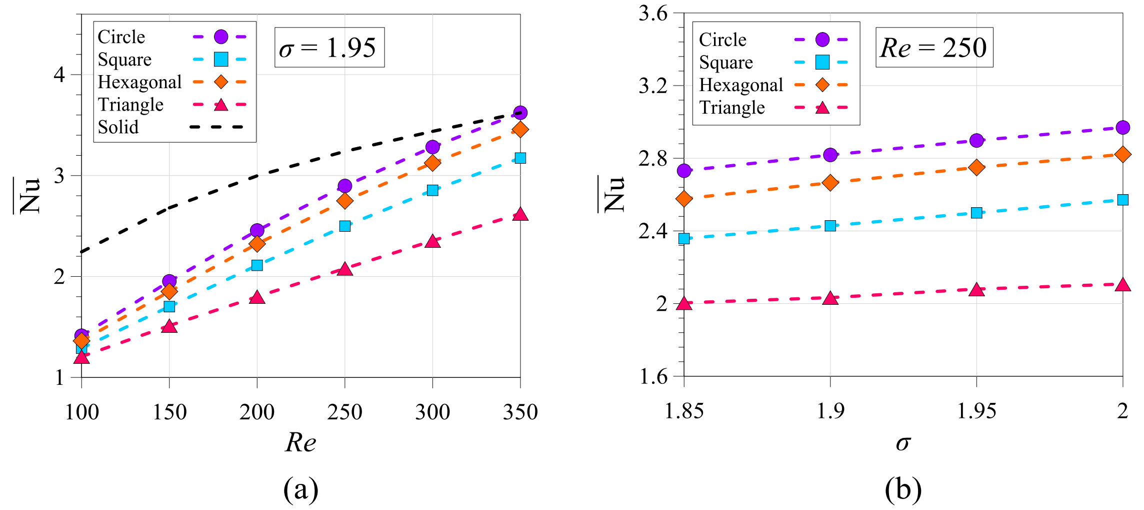

(a) (b)

Fig. 3 Variation of the average Nusselt number for different types of fin at various (a) Reynolds number and (b) surface area ratio

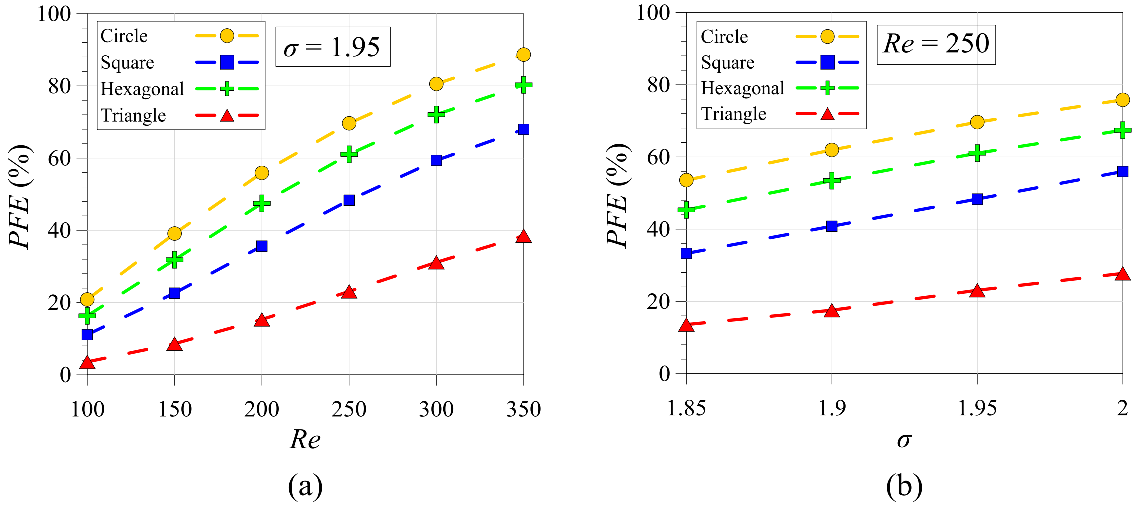

(a) (b)

Fig. 4 Variation of PFE for different types of fins at various (a) Reynolds number and (b) surface area ratio

5. CONCLUSIONS

This study presents an attempt to improve the thermal and hydraulic performance of fluid flow over a three-dimensional array of rectangular perforated fins with different perforation shapes and sizes. Flow and heat transfer characteristics were presented for Reynolds number (based on fin thickness) from 100 to 350, fin surface area ratio from 1.85 to 2 and different perforation shapes including circular, hexagonal, square, and triangular. The key conclusions are:

(1) Among the perforated fins, the lowest total drag force was observed for fins with circular perforations.
(2) The highest Nusselt number was observed for the solid fin. However, among perforated fins, the fin with triangular and circular perforations showed the lowest and highest Nusselt numbers, respectively.
(3) The highest perforated fin effectiveness (PFE) for equal fin surface area ratio was observed for fins with circular perforations.
(4) For the studied perforated fins, increasing Reynolds number and perforations size led to thermal performance enhancement.

NOMENCLATURE

ΔA	area	(m^2)	u	velocity component in X direction	(m/s)
C_p	specific heat at constant pressure	(J/kg K)	v	velocity component in Y direction	(m/s)
D	fin thickness	(m)	w	velocity component in Z direction	(m/s)
F_F	friction drag	(N)	Subscripts		
F_P	pressure drag	(N)	*DS, US*	downstream and upstream	
F_T	total drag	(N)	*in*	inlet	
h	heat transfer coefficient	(W/m^2 K)	S	surface of the fin	
H	fin height	(m)	*SF, PF*	solid and perforated fin	
K	thermal conductivity of fluid	(W/m K)	∞	free stream	
Nu	Nusselt number	(-)	Greek symbols		
P	air pressure	(Pa)	μ	air viscosity	(kg/m s)
q_f	heat transfer rate from the fin	(W)	ρ	air density	(kg/m^3)
Re	Reynolds number	(-)	σ	surface area ratio	(-)
T	temperature	(K)	τ_w	wall shear stress	(Pa)

REFERENCES

[1] Hajabdollahi, Z., Hajabdollahi, H., Fu, P.F., "Improving the rate of heat transfer and material in the extended surface using multi-objective constructal optimization," *International Journal of Heat and Mass Transfer,* 115, pp. 589-596, (2017).

[2] Hajmohammadi, M., Maleki, H., Lorenzini, G., Nourazar, S., "Effects of Cu and Ag nano-particles on flow and heat transfer from permeable surfaces," *Advanced Powder Technology,* 26(1), pp. 193-199, (2015).

[3] Maleki, H., Safaei, M.R., Alrashed, A.A., Kasaeian, A., "Flow and heat transfer in non-Newtonian nanofluids over porous surfaces," *Journal of Thermal Analysis and Calorimetry*, pp. 1-12, (2018).

[4] Maleki, H., Safaei, M.R., Togun, H., Dahari, M., "Heat transfer and fluid flow of pseudo-plastic nanofluid over a moving permeable plate with viscous dissipation and heat absorption/generation," *Journal of Thermal Analysis and Calorimetry*, pp. 1-12, (2018).

[5] Park, H.-K., Chung, B.-J., "The influence of tip clearance and Prandtl number on turbulent forced convection heat transfer of rectangular fins," *Heat and Mass Transfer,* 52(12), pp. 2759-2768, (2016).

[6] Zadhoush, M., Nadooshan, A.A., Afrand, M., "Constructal optimization of longitudinal and latitudinal rectangular fins used for cooling a plate under free convection by the intersection of asymptotes method," *International Journal of Heat and Mass Transfer,* 112, pp. 441-453, (2017).

[7] Ghorbani-Tari, Z., Chen, Y., Liu, Y., "End-wall heat transfer of a rectangular bluff body at different heights: Temperature-sensitive paint measurement and computational fluid dynamics," *Applied Thermal Engineering,* 122, pp. 697-705, (2017).

[8] Mokhtari, M., Gerdroodbary, M.B., Yeganeh, R., Fallah, K., "Numerical study of mixed convection heat transfer of various fin arrangements in a horizontal channel," *Engineering science and technology, an international journal,* 20(3), pp. 1106-1114, (2017).

[9] Maji, A., Bhanja, D., Patowari, P., Choubey, G., Deshamukhya, T., "Computational investigation of heat transfer analysis through perforated pin fins of different materials," *AIP Conference Proceedings*, vol. 1859, no. 1, p. 020009, (2017).

[10] Chidambaram, B., Ravichandran, M., Seshadri, A., Muniyandi, V., "Computational Heat Transfer Analysis and Genetic Algorithm–Artificial Neural Network–Genetic Algorithm-Based Multiobjective Optimization of Rectangular Perforated Plate Fins," *IEEE Transactions on Components, Packaging and Manufacturing Technology,* 7(2), pp. 208-216, (2017).

[11] Shaeri, M.R., Bonner, R., "Heat transfer and pressure drop in laterally perforated-finned heat sinks across different flow regimes," *International Communications in Heat and Mass Transfer,* 87, pp. 220-227, (2017).

[12] Shaeri, M., Yaghoubi, M., "Thermal enhancement from heat sinks by using perforated fins," *Energy conversion and Management,* 50(5), pp. 1264-1270, (2009).

[13] Shaeri, M.R., Jen, T.-C., "The effects of perforation sizes on laminar heat transfer characteristics of an array of perforated fins," *Energy Conversion and Management,* 64, pp. 328-334, (2012).